Available online at www.sciencedirect.com
SCIENCE DIRECT®
Polymer 44 (2003) 5015–5021
polymer
www.elsevier.com/locate/polymer

Crystalline structures in ultrathin poly(ethylene oxide)/poly(methyl methacrylate) blend films

Mingtai Wang*, Hans-Georg Braun*, Evelyn Meyer

Institute of Polymer Research Dresden, Hohe Strasse 6, D-01069 Dresden, Germany

Received 26 May 2003; received in revised form 2 June 2003; accepted 10 June 2003

Abstract

Amorphous poly(ethylene oxide)/poly(methyl methacrylate) (PEO/PMMA) blend films in extremely constrained states are meta-stable and phase separation of fractal-like branched patterns happens in them due to heterogeneously nucleated PEO crystallization by diffusion-limited aggregation. The crystalline branches are viewed flat-on with PEO chains oriented normal to the substrate surface, upon increasing PMMA content the branch width remains invariant but thickness increases. It is revealed that PMMA imposes different effects on PEO crystallization, i.e. the length and thickness of branches, depending on the film composition.

Keywords: Crystallization; Poly(ethylene oxide); Surface pattern

1. Introduction

Even though polymer crystallization has been extensively studied during the past decades [1,2], the crystallization in ultrathin films is a new topic in this field. Special enthalpic and entropic factors at polymer/substrate interface cause the organization of polymer chains in ultrathin films to deviate from their bulk states [3–6], and substrate adsorption effect, due to which polymer chains form stable loops dangling in the direction perpendicular to the substrate surface, reduces the thermodynamic potential of heterogeneous nucleation for crystallization [7]. Studying the crystallization in ultrathin polymer films has offered a possibility to reveal polymer chain organization during crystallization in real space [8–15]. However, observation of crystalline morphology has mainly been done in ultrathin films containing only one polymer, and branched structures due to non-equilibrium crystallization by a diffusion-limited aggregation (DLA) process are always the case in the films of a thickness less than 10 nm, as shown by the terrace structures with fingers [8,9], the finger-like [10–13] and fractal-like [15] patterns. In forming these structures, heterogeneous nucleation is necessary and polymer chains fold without influence of other polymers and by a stem length of 7–13 nm. In this report we show the crystalline structures in ultrathin poly(ethylene oxide)/poly(methyl methacrylate) (PEO/PMMA) blend films and the effects on PEO crystallization imposed by PMMA.

2. Experimental

Polyethylene glycol standard ($M_w = 6000$, $M_w/M_n = 1.03$) from Fluka and PMMA standard ($M_w = 4200$, $M_w/M_n = 1.06$) from Polymer Standards Services (PSS, Germany) were used as received to prepare PEO/PMMA blend films. The radius of gyration, R_g, of a polymer chain is calculated by $R_g = (Nb^2/6)^{1/2}$, where N is the degree of polymerization and b the average statistical segment length. For $b_{PMMA} = 0.69$ nm [16], the R_g of the PMMA chain is 1.77 nm. According to the data in literature [17], the b_{PEO} and R_g of the PEO chain are calculated to be 0.70 and 3.30 nm, respectively. Au films of 100 nm thickness were prepared by thermal evaporation (rate 0.1 nm/s) of gold on the glass slides primed with a Cr adhesive layer of 3 nm thickness. PEO/PMMA blend films were dip-coated on the Au films from chloroform solutions (totally 1 mg/ml) at an average lifting rate of 1.90 mm/s. The coated polymer layers (given a refractive index of 1.5)

* Corresponding authors. Tel.: +49-351-4658633; fax: +49-351-4658284.
E-mail addresses: mingtaiwang@hotmail.com (M. Wang), braun@ipfdd.de (H.G. Braun).

0032-3861/03/$ - see front matter © 2003 Elsevier Science Ltd. All rights reserved.
doi:10.1016/S0032-3861(03)00492-0

had a thickness (D) of 2–3.0 nm within the tested composition range (0–50% PMMA, by weight). For $D \leq R_g$ of the longest component (PEO), the films can be defined as extremely constrained two-dimensional ones [16,18].

To provide defined areas for studying crystallization by means of scanning electron microscopy (SEM) and atomic force microscopy (AFM), an newly-coated film was first scratched once with a razor blade after drying in the air for 15 min, and then put immediately into a vacuum (in SEM sample chamber, ca. 10^{-6} h Pa) to crystallize for about 17 h. For grazing incidence reflection infrared (GIR-IR) spectroscopy, the films that had been dried in the air for 15 min were crystallized in the vacuum for 24 h without scratching. The temperature in the vacuum chamber was estimated by ambient temperatures to be 21–22 °C. In vacuum condition the moisture influence on crystallization was eliminated.

Film thickness was measured on an ELX-02C ellipsometer (DRE GmbH, Germany; He–Ne laser source 632.8 nm, 70° angle of incidence) in 15–20 min after coating when the film was still amorphous. GIR-IR spectra were recorded in vacuum on an IFS66V/S spectrometer (Bruker Co.), using a grazing incidence external reflection stage (from SPECAC, incident angle 80 °C) at a resolution of 4 cm^{-1} and 1000 scans and a bare Au film as reference. Optical microscopy (OM) observation was done on a light microscope (Zeiss/Sis, Germany) in dark-field mode in ambient conditions. SEM and AFM studies of the samples were performed immediately after crystallization, as described previously [15].

3. Results

As a typical blend system containing amorphous and semi-crystalline components, PEO/PMMA blend in bulk state has been studied by different means, such as differential scanning calorimetry (DSC) [19], nuclear magnetic resonance (NMR) [20], small-angle X-ray scattering (SAXS) and small-angle neutron scattering (SANS) [21] and microscopy [22]. In general, PEO and PMMA are miscible in melt and amorphous states resulting in a single concentration-dependent glass transition [23], addition of PMMA reduces the crystal growth rate [24,25] and crystallinity [22,26] of PEO. The growth and melting of crystal lamellae of PEO spherulites in thin PEO/PMMA films have been revealed by hot-stage AFM [27]. Recently, Ferreiro and co-workers [28] reported that the crystalline morphology in thin PEO/PMMA films (ca. 200 nm thick) can be tuned by film composition to get circular spherulites (50–100% PEO), seaweed morphology (40–50% PEO), symmetric dendrites (30–40% PEO) and fractal structures (15–25% PEO). They also presented the growth dynamics of the symmetric dendrites with a focus on their growth pulsations [29], but how the film morphology is tuned by adding PMMA still remains unclear. In spite of the above extensive studies, we, to our knowledge, are still lacking the observation on the crystalline morphology in ultrathin PEO/PMMA films.

3.1. SEM and OM observations

After crystallization in vacuum for several hours (e.g. 17–18 h), the blend films are decorated by branched structures stemming from the scratch line (Fig. 1). The branched structures clearly resemble the fractals formed in electrodeposition [30,31] and bacterial growth [32]. Fractal formation proceeds theoretically by DLA process [33,34]. Crystalline structures reminiscent of DLA process have been observed in ultrathin PEO films, for example, the finger-like pattern in PEO monolayers [10,11]. Reasonably, the fractal-like structures here are related to PEO crystallization in the blend films by DLA process. Note that SEM observations of the fresh films showed that the PEO/PMMA films were homogeneous, but the pure PEO film was dispersed with some PEO dots (ca. 1 μm in diameter and 6–7 nm in height) that should be due to de-wetting of PEO on the substrate during film formation because of the weak interaction between the Au surface and PEO [35]; the non-scratched films were not found branched structures for at least 1 h when kept in the vacuum.

The branch growth depends strongly on film composition (Fig. 1). Generally, both main branches and sub-branches became shorter with PMMA content. The branches were very long in 90/10 (= PEO/PMMA) film, and the substrate surface was covered mainly by the branches stemming from the scratch line (Fig. 1(b)); but the branches in 75/25 film were much shorter than those in 90/10 film and a large structureless area appeared in front of the branches (Fig. 1(c)). Further increasing PMMA content to 40%, the branches along the scratch line became much shorter and a much larger structureless areas resulted in front of them (Fig. 1(d)). In PEO film, the branches stemming from PEO dots were much longer than these from the scratch line, the substrate surface was mainly covered by the branches nucleated by PEO dots which should crystallize prior to the branch growth because of their higher thickness [11].

The scratch line was created for two purposes, to act as heterogeneous nucleation for crystallization and to provided defined areas for studying crystallization. Under an optical microscope, 90/10 film was observed to show, in about 3 min after scratching with a needle (22 °C, 33% relative humidity), the contrast change in the zones along the scratch line, indicating the starting of crystallization; however, we didn't find evidently the crystal growth in 75/25 film for 25 min after scratching. Therefore, the branched structures here were not a direct result of scratching [36], and the scratch line acted as a surface defect to nucleate polymer chains. In the case of 50/50 film, where the branches were normally very short, a fortuitous long branched structure was found stemming from the scratch line, as shown in Fig. 2. SEM revealed that the long structure grew actually along a defect zone on the Au surface, which shows that the

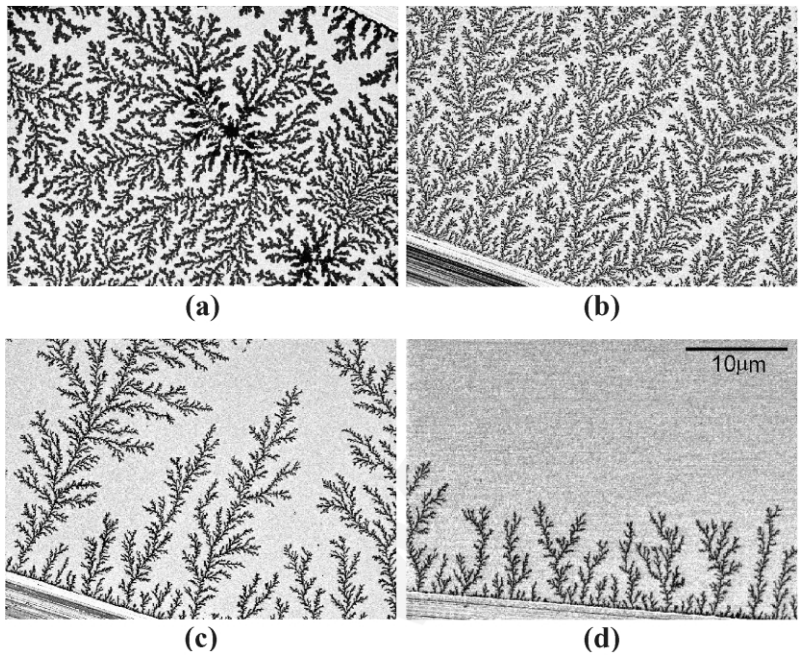

Fig. 1. SEM images of the fractal-like structures in ultrathin PEO/PMMA films of different blend compositions, (a) 100/0, (b) 90/10, (c) 75/25 and (d) 60/40. The scale bar of 10 μm is for all images. The samples were crystallized for 17 h.

structureless areas in front of the branches along the scratch line (Figs. 1(d) and 2) consist of amorphous PMMA and PEO but the crystallization in them needs further heterogeneous nucleation.

The crystallization in the films (Fig. 1) did take place in vacuum. On one hand, the time interval between the finish of scratching and the start of SEM vacuumization was very short (within ca. 1 min). On the other hand, if branch growth had finished before putting the film into the vacuum the branches should mainly stem from the scratch line and those nucleated by PEO dots should be much shorter in PEO film (Fig. 1(a)).

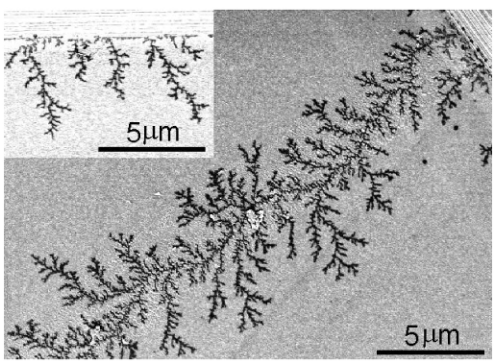

Fig. 2. A SEM image of the fractal-like structures in ultrathin PEO/PMMA film of 50/50 composition. The branches along the scratch line are normally very short in this sample (Inset). This image mainly shows a long branched structure stemming from the scratch line, which grew actually along a defect zone. The sample was crystallized for 17.5 h.

3.2. GIR-IR measurements

Fig. 3 shows the GIR-IR spectra of the ultrathin films. Detailed assignments of IR vibrations of PEO [35,37] and PMMA [38] have been described by others. Compared with the isotropic spectrum of bulk PMMA, the stretching band of methacrylate side group at 1100–1300 cm^{-1} is greatly enhanced relative to the C=O vibration at 1734 cm^{-1} in the ultrathin PMMA film, indicating that the film has more methoxy groups oriented normal to the Au surface than carbonyl groups and that PMMA is physically adsorbed onto the substrate due to interaction of the polar methoxy

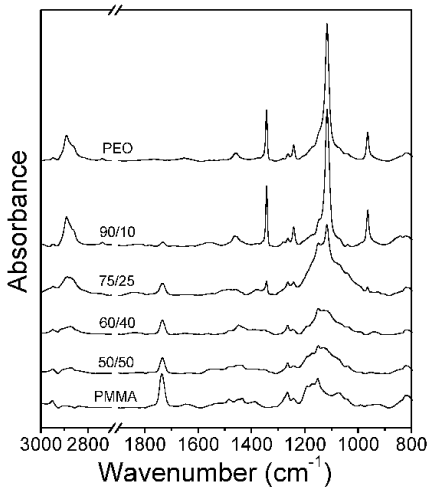

Fig. 3. GIR-IR spectra of the ultrathin films crystallized for 24 h. The traces correspond to the weight ratios of PEO/PMMA marked on the curves. SEM verified that the crystallization in blend films started from surface defects (e.g. dust particles).

and carbonyl groups with the Au surface [38]. Reasonably, PMMA prevented PEO from de-wetting during the co-deposition of them from solution [35], resulting in homogeneous blend films.

The spectra of PEO at different temperatures [35,37] show that the intensity of the CH_2 wagging vibration of PEO at 1342 cm^{-1} is sensitive to the conformation order, which can be used to evaluate crystallization process [26]. With respect to the CH_2 stretching vibration at around 2888 cm^{-1} that is mainly attributed to PEO component, the change in the intensity of PEO band at 1342 cm^{-1} with PMMA content indicates that a higher PMMA content leads to a lower crystallinity of PEO in the film. As PMMA content is $\geq$40% the blend films are mainly amorphous.

Only bands with transition dipole moments parallel (‖) to PEO chain axis (1342, 1242, 1107 and 963 cm^{-1}) [35,37] are intensively observed in the GIR-IR spectra of ultrathin PEO and 90/10 films. In the spectrum of 75/25 film, the vibrations of ‖ bands are still evident while they are much weaker than the 90/10 and PEO cases. In the films with PMMA content $\geq$40% the vibration signals of PEO crystals are very weak (1342 cm^{-1}) and non-evident (963 cm^{-1}) for the crystal branches in them were too short to be easily detected by the GIR-IR scans, but the orientation of the crystallized PEO chains in them can be reasonably inferred by the results of the 90/10 and 75/25 films since the films crystallized in the same condition. Thus, the PEO chains in the crystals formed in the studied films orient perpendicular to substrate surface and the branches are viewed flat-on, because in GIR-IR measurements only the transition dipole moment components normal to substrate surface can be observed.

3.3. AFM results

AFM measurements were performed to get the branch thickness, as shown in Fig. 4. In the PEO film, the branches had a homogeneous thickness of 8 ± 1 nm (Fig. 4(a)). However, the branch thickness in the blend films verified with PMMA content, namely, 4 ± 1 nm in 90/10 film (Fig. 4(b)), 6 ± 1 nm in 75/25 film (Fig. 4(c)) and 10 ± 1 nm in 60/40 and 50/50 films (Fig. 4(d)). For PMMA phases may segregate beside the branches (refer to latter discussion), the actual branch thickness may be somewhat larger than the measured data in the blend films, particularly in those containing a high PMMA content. Notice that the branches in 60/40 and 50/50 films had a similar thickness by the AFM data (Fig. 4(d)), but the branches in the 50/50 film may actually be thicker than those in 60/40 film because more PMMA can segregate beside the branches in 50/50 film.

As the branch growth mainly proceeds laterally and the PEO chains within the crystals take exclusively a conformation with chain axes perpendicular to substrate surface, one branch formed in the films studied here is reasonably a crystal lamella viewed flat-on and its thickness is related to the stem length of PEO chain folds within it. In pure PEO film the thickness of such branches is a direct measure of chain folding states [11,12,15]. The thickness of 8 ± 1 nm (Fig. 4(a)) infers that PEO chains fold 4 times when without influence of PMMA, as the length L of the fully extended crystalline PEO chain is 37 nm according to $L = (M_n^{PEO}/M_n^{EO}) \times 0.2783$ nm [39]. Even though the exact folding states of PEO chains in blend films, particularly as a film contains a high PMMA content, are hard to obtain from the AFM data (Fig. 4(c) and (d)) because of the possible discrepancy between the actual and measured values of the branch thickness, the tendency towards higher branches when increasing PMMA content will not be altered. Therefore, from the composition dependence of branch thickness one would get an evaluation of PMMA influences on the organization of PEO chains during crystallization.

4. Discussion

The amorphous PEO/PMMA blend films are obtained by constrained geometry and only meta-stable, phase separation of fractal-like branched patterns happens in them due to heterogeneously nucleated PEO crystallization by DLA process. The PEO chains in the crystals come from the amorphous blend areas ahead of them [10–12,15], where PEO and PMMA are mixed. Results show that increasing PMMA content to more than 10% leads to a remarkable retardation effect of PMMA on the branch length, and only the PEO chains near the heterogeneous nucleation sites in films with PMMA content $\geq$40% can crystallize so that the films are mainly amorphous (Figs. 1–3). In bulk state, the blends with PMMA content higher than ~70% are completely amorphous [19,22,40]. This indicates that the retardation effect of PMMA on PEO crystallization is dramatically enhanced by constrained geometry in the ultrathin films.

Crystallization in the blend films involves the general features revealed in ultrathin PEO [10–12,15] and other polymer [8,9,14] films, namely, requiring necessary heterogeneous nucleation, chain orientation normal to substrate surface and branched structures related to DLA process. Therefore, the crystal growth in the blend films obeys the basic principles in ultrathin polymer films, for example, the growth process is controlled by chain diffusion. It is believed that the retardation effect of PMMA on the branch growth is to reduce the transport property (mobility) of PEO chains in our cases, because upon increasing PMMA the mobility of PEO chains can be strongly reduced [20] and the system will become more rigid [22].

SEM and AFM provide detailed structural information on the crystals. These data contain several interesting features. First, as PMMA content was changed from 10 to 40%, the branch thickness increased strikingly from 4 ± 1 to 10 ± 1 nm. Second, the branches in 90/10 film were much thinner than those in PEO film. Finally, the branch

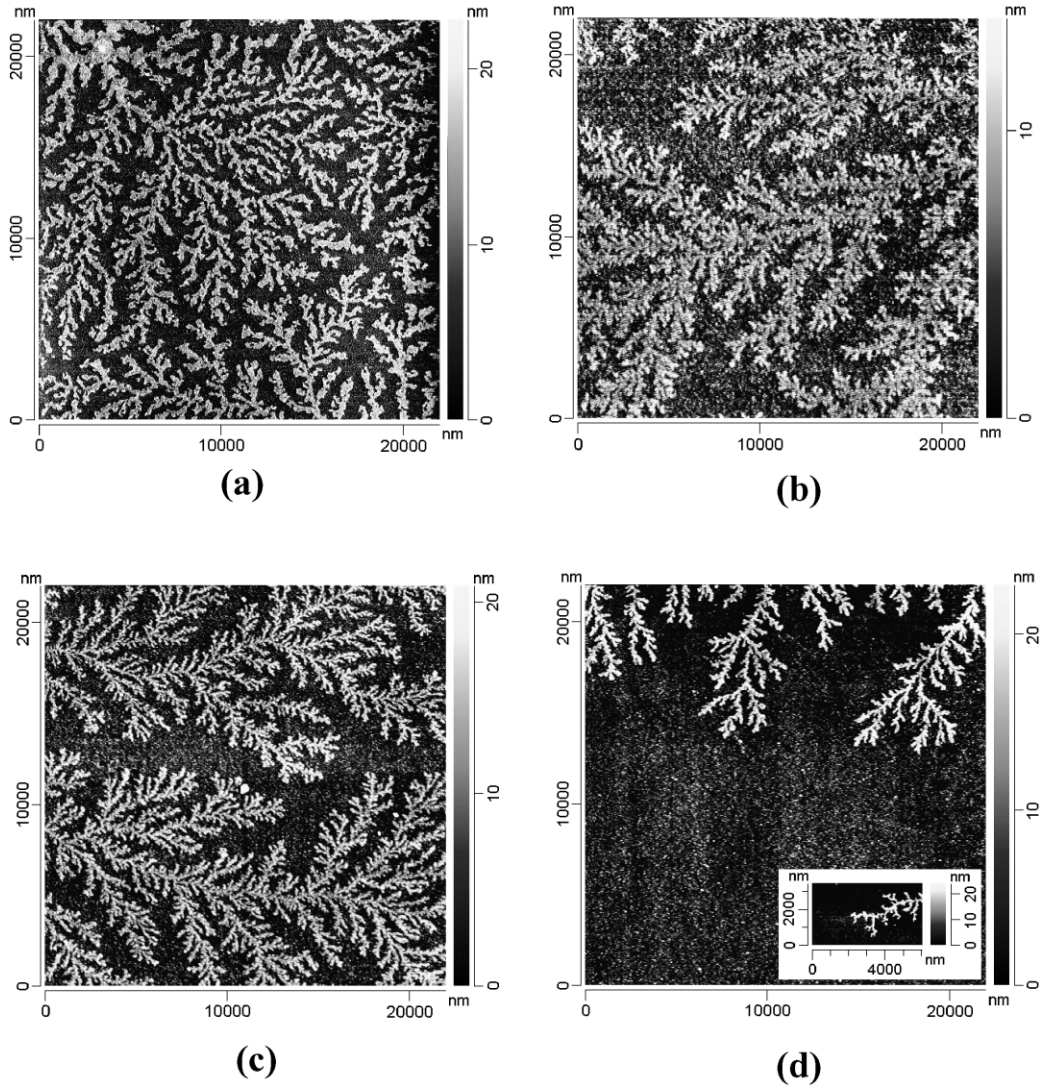

Fig. 4. AFM images of the fractal-like structures in ultrathin PEO/PMMA films of different blend compositions, (a) 100/0, (b) 90/10, (c) 75/25 (c) and (d) 60/40. The inset to (d) is for 50/50 film. The samples were crystallized for 17 h and measured by means of non-contact AFM immediately after being taken out of the vacuum chamber; the scanned areas were near scratch line. All the branches were nucleated by the scratch lines, except for those in the left side of image (a) that were nucleated by a PEO dot.

width (ca. 0.20 μm) in the blend films was independent of PEO/PMMA ratio, but smaller than that of the branches formed in the PEO film. As mentioned previously, the branch thickness is directly related to the chain folding during crystallization and can give an access to the information on the organization of PEO chains under PMMA influence.

The thickness of the crystalline branches is determined by the kinetics of chain deposition at crystal growth fronts in diffusion-controlled growth process [11,12,15]. A lowered chain deposition rate, which was achieved by evaluating crystallization temperature (T_c) [11] and by reducing the polymer concentration in diffusion field [15], has been proved in ultrathin PEO films to favor the growth of thicker branches. Reiter and Sommer [11,12] showed that the thickness of crystal lamellae increases with crystallization temperature. They argued that at a high deposition rate (large undercooling) the molecules attached to the crystal have less time to stretch out and are thus in a state of relatively low internal chain order (folded state); in contrast, if the crystals grow slowly, the attached molecules have more time to relax towards the fully extended form of lowest free energy by rearrangements at the crystal surface. Our previous results [15] showed that, as a result of the reduction of chain availability in the diffusion field, the chain deposition rate (or probability) at crystal growth fronts becomes small and the deposited polymer chains have a high probability to rearrange themselves to a state near equilibrium.

In our opinion, the increase in branch thickness with PMMA content in the blend films results from the lowered chain deposition rate by adding PMMA (Fig. 4(b)–(d)). PMMA has a high glass transition temperature (T_g), but PEO have a low one. As a consequence of mixing these two

miscible polymers, the amorphous phase T_g increases as the concentration of PMMA increases [23], resulting in a more rigid crystallization system with a more reduced mobility of PEO chains. The reduction of PEO chain mobility will inevitably lower the chain deposition rate at crystal growth fronts, leading to an easier relaxation of the deposited chains towards the extended state and further higher branches as described elsewhere [11,15].

In a blend consisting of a semi-crystalline polymer and an amorphous one the equilibrium melting point ($T_m^{o\prime}$) depends on composition, increasing amorphous concentration will depress $T_m^{o\prime}$ [24,41,42]. One question may arise, concerning whether the origin of the increase in branch thickness with PMMA content comes from the decrease in the effective undercooling ΔT ($\Delta T = T_m^{o\prime} - T_c$) at which crystallization occurs. $T_m^{o\prime}$ in PEO/PMMA blends decreases with increase of PMMA content in the blends [24,41], but the decreases is slight and only a maximum depression of ca. 2.5 °C was observed [24]. In spite of the depression of $T_m^{o\prime}$, moreover, the crystalline thickness in PEO/PMMA blends is independent of composition [21,41], but increases with T_c. The equilibrium melting point (T_m^o) of the pure PEO used in this study was ca. 64 °C, which was obtained by referring to the data of a similar PEO ($M_w = 6000$, $M_w/M_n = 1.03$, from Fluka Co.) in literature [24]. There is no reason to believe that the increase in branch thickness with increasing PMMA content in our cases results mainly from the decrease in the effective undercooling, of which the contribution would be very faint if it could not be completely ruled out because the T_c in our experiments was about 42 °C below the T_m^o of the pure PEO.

Interestingly, the branches in 90/10 film were much thinner than those in PEO film (Fig. 4(a) and (b)), which should not be caused by the PMMA segregating beside the branches in the blend film because PMMA content was rather low. A slow deposition rate of PEO chains at growth fronts favors the formation of higher branches, whereas a fast deposition rate will result in thinner branches [11,15]. It is clear that the crystallization was accelerated in 90/10 film as compared with that in PEO film. The crystal growth was also found to be enhanced in 90/10 blend of PEO/isotactic-PMMA (*i*-PMMA) when compared to the pure PEO, rather than being disrupted, this phenomenon was considered to relate to the immiscibility between PEO and *i*-PMMA [25]. Therefore, two competitive effects may be imposed by PMMA on PEO crystallization depending on the film composition, to retard the crystallization by reducing the mobility of PEO chains and to accelerate the crystallization by probably de-mixing, where the latter effect is dominant as PMMA concentration is low but the former one will be enhanced by increasing PMMA content (Fig. 4).

As shown previously [15], a surface-tension effect, which favors the minimized interface area of crystal growth fronts, is coming into effect with the reduction in deposition rate of chains and the deposited chains will occupy a highest number of nearest neighbors at the growth fronts. With this consideration, one might expect a broadening of branches as the deposition rate reduces with increasing PMMA content. However, the branch width (ca. 0.20 μm) in the blend films is independent of film composition and generally smaller than that in PEO film (Figs. 1 and 4). No external factors could impose influences on the branch width in our experiments, except for the presence of PMMA in the system. On the other hand, the width difference between the branches in the blend and PEO films could not result from the two competitive effects imposed by PMMA in that the branch width did not changed with increasing PMMA content. The possible origin of the small and constant branch width in blend films lies in the laterally excluded PMMA phases from the crystals, which can be rationalized by the fact that the 'impurities' (PMMA) segregate away from the growth front and between the growing lamellae during the growth of PEO spherulites in thin PEO/PMMA films [27] and by the invariant crystalline lamellar thickness and increasing small-angle long period of crystalline phases with addition of PMMA [21,41]. The deposition of PEO chains at the side faces of branches can be prevented by the excluded PMMA phases, but this will not be the case in the PEO film.

5. Conclusion

The results presented in this study show the crystalline morphology in ultrathin PEO/PMMA blend films. The blend films in extremely constrained states are amorphous and meta-stable, and phase separation in them follows a fractal-like branched pattern due to heterogeneously nucleated PEO crystallization by DLA process. The crystal branches are viewed flat-on with polymer chains oriented normal to the substrate surface; the PEO chains in the crystalline branches come from the amorphous blend areas ahead of them. The branch width in blend films is independent of the film composition, which relates to the laterally excluded PMMA phases from the crystals. The presence of PMMA influences strikingly the branch length and thickness by imposing two competitive effects on the PEO crystallization, to accelerate and to retard the crystallization, depending on the film composition. The accelerated crystallization, probably by de-mixing between PEO and PMMA, leads to thinner and longer crystal branches; the retardation effect of PMMA, which results in thicker and shorter crystal branches, is attributed to reducing the mobility of PEO chains in the system.

Acknowledgements

The authors thank the DFG for supporting this work (priority program 'Wetting and structure formation at surfaces'). M. Wang acknowledges the Alexander von Humboldt Foundation for a research fellowship.

References

[1] Bassett BC. Principles of polymer morphology. Cambridge: Cambridge University Press; 1981.
[2] Strobl G. The physics of polymers. Berlin: Springer; 1996.
[3] Despotopoulou MM, Miller RD, Rabolt JF, Frank CW. J Polym Sci: Part B: Polym Phys 1996;34:2335–49.
[4] Despotopoulou MM, Frank CW, Miller RD, Rabolt JF. Macromolecules 1996;29:5797–804.
[5] Frank CW, Rao V, Despotopoulou MM, Pease RFW, Hinsberg WD, Miller RD, Rabolt JF. Science 1996;273:912–5.
[6] Theodotou DN. Molecular modeling of polymer surfaces and polymer/solid interfaces. In: Sanchez IC, editor. Physics of polymer surfaces and interfaces. Butterworth-Heinemann: Boston; 1992. p. 139–62.
[7] Ebengou RH. J Polym Sci: Part B: Polym Phys 1997;35:1333–8.
[8] Sakai Y, Imai M, Kaji K, Tsuji M. J Cryst Growth 1999;203:244–54.
[9] Sakai Y, Imai M, Kaji K, Tsuji M. Macromolecules 1996;29:8830–4.
[10] Reiter G, Sommer JU. Phys Rev Lett 1998;80:3771–4.
[11] Reiter G, Sommer JU. J Chem Phys 2000;112:4376–83.
[12] Sommer JU, Reiter G. J Chem Phys 2000;112:4384–93.
[13] Reiter G, Castelein G, Sommer JU. Phys Rev Lett 2001;86:5918–21.
[14] Zhang F, Liu J, Huang H, Du B, He T. Eur Phys J E 2002;8:289–97.
[15] Wang M, Braun HG, Meyer E. Macromol Rapid Commun 2002;23:853–8.
[16] Tanaka K, Takahara A, Kajiyama T. Macromolecules 1996;29:3232–9.
[17] Chen EQ, Lee SW, Zhang A, Moon BS, Mann I, Harris FW, Cheng SZD, Hsiao BS, Yeh F, von Merrewell E, Grubb DT. Macromolecules 1999;32:4784–93.
[18] Tanaka K, Yoon JS, Takahara A, Kajiyama T. Macromolecules 1995;28:934–8.
[19] Liau WB, Chang CF. J Appl Polym Sci 2000;76:1627–36.
[20] Schantz S. Macromolecules 1997;30:1419–25.
[21] Russell TP, Ito H, Wignall GD. Macromolecules 1988;21:1703–9.
[22] Martuscelli E, Silvestre C, Addonizio ML, Amelino L. Makromol Chem 1986;187:1557–71.
[23] Liberman SA, Gomes AS, Macchi EM. J Polym Sci: Polym Chem Ed 1984;22:2809–15.
[24] Alfonso GC, Russell TP. Macromolecules 1986;19:1143–52.
[25] John E, Ree T. J Polym Sci: Part A: Polym Chem 1990;28:385–98.
[26] Li X, Hsu SL. J Polym Sci: Polym Phys Ed 1984;22:1331–42.
[27] Pearce R, Vancso GJ. J Polym Sci: Part B: Polym Phys 1998;36:2643–51.
[28] Ferreiro V, Douglas JF, Warren JA, Karim A. Phys Rev E 2002;65:042802.
[29] Ferreiro V, Douglas JF, Warren J, Karim A. Phys Rev E 2002;65:051606.
[30] Matsushita M, Sano M, Hayakawa Y, Honjo H, Sawada Y. Phys Rev Lett 1984;53:286–9.
[31] Matsushita M, Hayakawa Y, Sawada Y. Phys Rev A 1985;32:3814–6.
[32] Ben-Jacob E. Contemporary Phys 1997;38:205–41.
[33] Witten TA, Sander LM. Phys Rev Lett 1981;47:1400–3.
[34] Sander LM. Nature 1986;322:789–93.
[35] Hoffmann CL, Rabolt JF. Macromolecules 1996;29:2543–7.
[36] Hobbs JK, Humphris ADL, Miles MJ. Macromolecules 2001;34:5508–19.
[37] Yoshihara T, Tadokoro H, Murahashi S. J Chem Phys 1964;41:2902–11.
[38] Lenk TJ, Hallmark VM, Rabolt JF, Häussling L, Ringsdorf H. Macromolecules 1993;26:1230–7.
[39] Kovacs AJ, Straupe C. J Cryst Growth 1980;48:210–26.
[40] Parizel N, Lauprêtre F, Monnerie L. Polymer 1997;38:3719–25.
[41] Cimmino S, Pace ED, Martuscelli E, Silvestre C. Makromol Chem 1990;191:2447–54.
[42] Rim PB, Runt JP. Macromolecules 1984;17:1520–6.